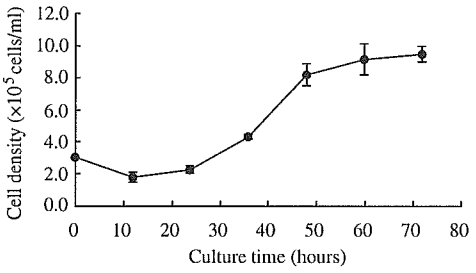

Fig. 7. Time course of cell density of FLAG-tagged prestin-expressing CHO cells cultured in CHO-S-SFM II medium. Cell density was counted with a hemocytometer every 12 h. Error bars show ± SD ($n = 4$).

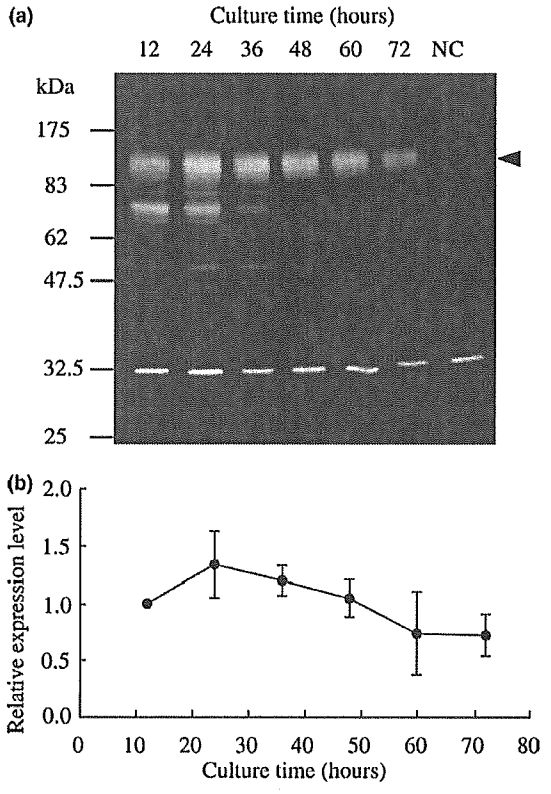

Fig. 8. Expression level of FLAG-tagged prestin in CHO cells cultured in CHO-S-SFM II medium. (a) Representative result of Western blot analysis. Cells (5×10^4) harvested every 12 h during the culture were loaded. Arrow indicates the prestin bands. NC: untransfected CHO cells. (b) Time course of the relative expression level of prestin. The expression levels in the cells at different points of time relative to that in the cells cultured 12 h after passage were evaluated from the luminescence intensity of Western blot bands. Error bars show ± SD ($n = 4$).

be expressed in CHO cells. As the composition and constitution of the membrane of *E. coli* are generally recognized to be quite different from those of the mammalian plasma membrane, we did not expect prestin to be expressed in the membrane of *E. coli*. We alternatively expected that prestin, which is a hydrophobic membrane protein, would be expressed as an inclusion body using the pET28b expression vector or as a solubilized protein fused with hydrophilic MBP using the pMAL-c2 expression vector. Contrary to expectations, however, prestin was not expressed in these cells at all. It is presumed that prestin is toxic for *E. coli*.

In our Western blot analysis (Fig. 1), when the baculovirus expression system was used, a band around 65 kDa and some weak bands below that were detected in transfected cells, while no band was detected in untransfected cells. The band around 65 kDa represents prestin and the other lighter bands are likely to represent fragments of prestin. On the other hand, when the CHO expression system was used, a band around 90 kDa representing prestin was detected in transfected cells. Bands around 30 kDa detected in both transfected CHO cells and untransfected CHO cells may have resulted from nonspecific binding of antibodies. The difference between the band around 90 kDa, characterized by broadness and brightness, detected in CHO cells and the band around 65 kDa, characterized by sharpness, detected in Sf9 cells suggests that prestin expressed in CHO cells is glycosylated while that in Sf9 insect cells is not. As prestin expressed in CHO cells is modified by different lengths of carbohydrate chains, prestin expressed in CHO cells is heavier than that in Sf9 cells and varies in molecular weight. As a result, the position of the band detected in CHO cells is higher than that detected in Sf9 cells, and the band detected in CHO cells is broad. Stabilization of prestin would also be realized by glycosylation, which may lead to a high level of expression of prestin in CHO cells. As a result, the band detected in CHO cells was brighter than that detected in Sf9 cells. The idea that prestin is glycosylated in CHO cells agrees with a glycosylation study of prestin reported by Matsuda et al. (2004).

In our experimental results, prestin was not expressed in *E. coli* at all and only slightly expressed in insect cells. However, since few attempts were made to express prestin in insect cells and bacterial cells, there is a possibility that it could be expressed in such cells using other host vector systems. Even though there are other possibilities to obtain prestin, we adopted the CHO cell expression system because prestin was well expressed in CHO cells.

Transfected cell lines were obtained by limiting dilution cloning, and GFP was stably expressed for over 4 months in these cell lines. As the prestin gene and the GFP gene are transcribed into sequential mRNA when the constructed expression vector is used, stable expression of prestin may be achieved in these cell lines. In fact, according to the results of immunofluorescence experiments shown in Fig. 2, it was confirmed that FLAG-tagged prestin was stably expressed in the generated cell line after subculturing for 4 months. As the same expression vector was applied, it was anticipated that wild-type prestin was also stably expressed in the

generated cell line. We therefore considered that the stable prestin-expressing cell lines have been established using transfected CHO cells.

The electrophysiological properties of the OHCs measured in this study agree with those of OHCs reported by Huang and Santos-Sacchi (1993), and the electrophysiological properties of prestin-expressing CHO cells, which were subcultured for over 4 months and measured in this study, agree with those of transiently prestin-expressing CHO cells reported by Ludwig et al. (2001). As both the established wild-type prestin-expressing and FLAG-tagged prestin-expressing cell lines exhibited bell-shaped nonlinear membrane capacitance fitted to Eq. (4), similar to prestin in the OHCs, wild-type prestin and FLAG-tagged prestin expressed in the established cell lines have activity. Moreover, as there were no significant differences between the electrophysiological properties of wild-type prestin-expressing cells and those of FLAG-tagged prestin-expressing cells, it is concluded that the FLAG-tag does not interfere with the function of prestin (Table 1). FLAG-tagged prestin can therefore be applied to the study of prestin.

Nonlinear membrane capacitance was not obtained in about half of the transfected cells. The reason for this result may have been individual differences in the expression level of prestin in the transfected cells. When the expression level of prestin was low, it was difficult to obtain nonlinear membrane capacitance which fitted Eq. (4) with a correlation coefficient of $R \geqslant 0.98$ because the measured membrane capacitance was affected by measurement noise. If measurement noise were decreased, more cells would show nonlinear capacitance. Although about half of the transfected cells do not show nonlinear capacitance, i.e., the expression level of prestin in some cells is low, it does not interfere with obtaining prestin from those cells.

The expression level of prestin in the established cell line was then estimated using the obtained linear capacitance, C_{lin}, and the maximum charge transfer, $Q_{\max}$. As $Q_{\max}$ indicates the total amount of charge carried by all prestin in the plasma membrane and e is electron charge, which is presumed to equal the charge carried by one prestin molecule, the number of prestin molecules in the cell is given by $Q_{\max}/e$. As C_{lin} expressed in picofarads indicates the total capacitance of the plasma membrane of the cell, and the membrane capacitance of the cell per unit surface area is known to be 0.01 pF/μm^2 (Neher and Marty, 1982), the surface area of the cell is expressed by $C_{\mathrm{lin}}/0.01$ μm^2. The expression level of prestin per unit surface area, i.e., charge density, of the cell can therefore be obtained with

$$\text{Charge density} = \frac{Q_{\max}}{e} \Big/ \frac{C_{\mathrm{lin}}}{0.01}. \tag{6}$$

The charge density of the 20 measured wild-type prestin-expressing CHO cells and 19 measured FLAG-tagged prestin-expressing CHO cells were determined to be 246 ± 125 and 255 ± 88 μm^{-2}, respectively (Table 1). The charge densities of established cell lines are lower than the average density of OHCs, which is 6830 μm^{-2} as obtained in this study or 7500 μm^{-2} as reported by Huang and Santos-Sacchi (1993). The charge densities are also lower than that of transiently prestin-expressing TSA201 cells, reported to be 5360 μm^{-2} by Zheng et al. (2000). Although the expression levels were 1/20–1/35 of those in OHCs and TSA201 cells, the stable expression of prestin in the established cell lines is an advantage.

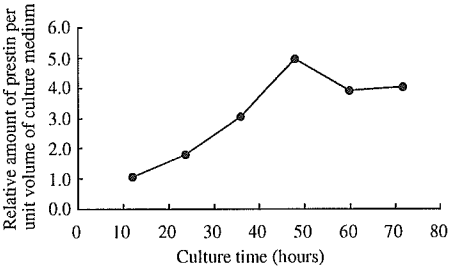

Fig. 9. Time course of the relative values of the amount of prestin in unit volume of culture medium. The amount of prestin included in unit volume of culture medium was the result of multiplication of the cell density by the relative expression level. Values were normalized to the value of 12 h after passage.

To obtain prestin efficiently, the optimal culture conditions for an established cell line was considered. Generally, suspension culture is advantageous for obtaining a large number of cells because cell number per unit volume of medium can be raised by use of a three-dimensional culture rather than a monolayer culture, and culture procedures are manageable. The established FLAG-tagged prestin-expressing cells were therefore cultured in CHO-S-SFM II medium to achieve growth of suspension cells. The cells cultured as suspension cells also exhibited a bell-shaped nonlinear membrane capacitance, i.e., prestin expressed in suspension cells has activity. When prestin is researched at the molecular level, the percentage of prestin in total proteins expressed in the cells, which is shown in Fig. 8(b), is an important factor because impurities interfere with the experimental procedure. The amount of prestin per unit volume of culture medium, which is shown in Fig. 9, is another important factor for efficient acquisition. This is obtained by multiplication of the cell density (Fig. 7) by the expression level (Fig. 8(b)). Fig. 8(b) demonstrates that the variation of the relative expression level is relatively small (from 0.7 to 1.3). By contrast, the relative amount of prestin per unit volume of culture medium increased from 1.0 up to 4.9 at 48 h after passage, and then decreased. From these results, it is concluded that cells should be harvested around 48 h after passage to efficiently obtain prestin.

5. Conclusions

In this study, to obtain a large amount of prestin, an expression system for prestin was constructed. The conclusions are as follows:

1. Prestin was expressed in mammalian cells, but not in *E. coli* nor in insect cells.
2. Prestin-expressing cell lines were generated by limiting dilution cloning. In these cell lines, although the expression levels were 1/20–1/35 of those in OHCs and of those in TSA201 cells transiently expressing prestin, prestin was expressed stably in the generated cell lines.
3. To obtain prestin efficiently, cells should be grown as suspension cells using CHO-S-SFM II medium, and be harvested at approximately 48 h after passage.

Acknowledgements

This work was supported by a grant from the Human Frontier Science Program, by a Health and Labor Science Research Grant from the Ministry of Health, Labor and Welfare of Japan, and by Grant-in-Aid for Scientific Research on Priority Areas 15086202 from the Ministry of Education, Culture, Sports, Science and Technology of Japan.

References

Ashmore, J.F., 1987. A fast motile response in guinea-pig outer hair cells: the cellular basis of the cochlear amplifier. J. Physiol. 388, 323–347.

Avgerinos, G.C., Drapeau, D., Socolow, J.S., Mao, J., Hsiao, K., Broeze, R.J., 1990. Spin filter perfusion system for high density cell culture: production of recombinant urinary type plasminogen activator in CHO cells. Biotechnology 8, 54–58.

Brownell, W.E., Bader, D., Ribaupierre, Y., 1985. Evoked mechanical responses of isolated cochlear outer hair cells. Science 227, 194–196.

Dallos, P., 1992. The active cochlea. J. Neurosci. 12, 4575–4585.

Forge, A., 1991. Structural features of the lateral walls in mammalian cochlea outer hair cells. Cell Tissue Res. 265, 473–485.

Frolenkov, G.I., Mammano, F., Belyantseva, I.A., Coling, D., Kachar, B., 2000. Two distinct Ca^{2+}-dependent signaling pathways regulate the motor output of cochlear outer hair cells. J. Neurosci. 20, 5940–5948.

Huang, G., Santos-Sacchi, J., 1993. Mapping of the distribution of the outer hair cell motility voltage sensor by electrical amputation. Biophys. J. 65, 2228–2236.

Kachar, B., Brownell, W.E., Altschuler, R., Fex, J., 1986. Electrokinetic shape changes of cochlear outer hair cells. Nature 322, 365–368.

Liberman, M.C., Gao, J., He, D.Z.Z., Wu, X., Jia, S., Zuo, J., 2002. Prestin is required for electromotility of the outer hair cell and for the cochlear amplifier. Nature 419, 300–304.

Ludwig, J., Oliver, D., Frank, G., Klöcker, N., Gummer, A.W., Fakler, B., 2001. Reciprocal electromechanical properties of rat prestin: the motor molecule from rat outer hair cells. Proc. Natl. Acad. Sci. USA 98, 4178–4183.

Matsuda, K., Zheng, J., Du, G.G., Klöcker, N., Madison, L.D., Dallos, P., 2004. N-linked glycosylation sites of the motor protein prestin: effects on membrane targeting and electrophysiological function. J. Neurochem. 89, 928–938.

Neher, E., Marty, A., 1982. Discrete changes of cell membrane capacitance observed under conditions of enhanced secretion in bovine adrenal chromaffin cells. Proc. Natl. Acad. Sci. USA 79, 6712–6716.

Oliver, D., He, D.Z.Z., Klöcker, N., Ludwig, J., Schulte, U., Waldegger, S., Ruppersberg, J.P., Dallos, P., Fakler, B., 2001. Intracellular anions as the voltage sensor of prestin, the outer hair cell motor protein. Science 292, 2340–2343.

Santos-Sacchi, J., 1991. Reversible inhibition of voltage-dependent outer hair cell motility and capacitance. J. Neurosci. 11, 3096–3110.

Santos-Sacchi, J., Dilger, J.P., 1988. Whole cell currents and mechanical responses of isolated outer hair cells. Hear. Res. 35, 143–150.

Santos-Sacchi, J., Shen, W., Zheng, J., Dallos, P., 2001. Effects of membrane potential and tension on prestin, the outer hair cell lateral membrane motor protein. J. Physiol. 531, 661–666.

Wu, X., Gao, J., Guo, Y., Zuo, J., 2004. Hearing threshold elevation precedes hair-cell loss in prestin knockout mice. Mol. Brain Res. 126, 30–37.

Zenner, H.P., 1986. Motile responses in outer hair cells. Hear. Res. 22, 83–90.

Zheng, J., Long, K.B., Shen, W., Madison, L.D., Dallos, P., 2001. Prestin topology: localization of protein epitopes in relation to the plasma membrane. NeuroReport 12, 1929–1935.

Zheng, J., Shen, W., He, D.Z.Z., Long, K.B., Madison, L.D., Dallos, P., 2000. Prestin is the motor protein of cochlear outer hair cells. Nature 405, 149–155.

Effects of Mutation in the Conserved GTSRH Sequence of the Motor Protein Prestin on Its Characteristics*

Shun KUMANO**, Koji IIDA**, Michio MURAKOSHI**,
Naoyuki NAITO**, Kouhei TSUMOTO***, Katsuhisa IKEDA****,
Izumi KUMAGAI†, Toshimitsu KOBAYASHI†† and Hiroshi WADA**

Prestin is a motor protein responsible for the outer hair cell (OHC) electromotility which amplifies the vibration of the organ of Corti in the inner ear. Identification of the functional significance of particular amino acids is necessary to characterize prestin. In this study, an attempt was made to clarify the role of the GTSRH sequence at positions 127–131 in prestin conserved in six proteins of the solute carrier (SLC) 26 family of which prestin is a member. To elucidate what role that sequence plays in the characteristics of prestin, mutations were introduced into the sequence and the characteristics of the constructed point mutants were investigated by Western blotting, immunofluorescence experiments and the whole-cell patch-clamp technique. The localization of T128A was altered, the anion transport function of H131A and that of S129T were lost and such functions of G127A, T128A, S129A and R130A declined. These results suggest that the GTSRH sequence plays an important role in the localization of prestin, as well as in its anion transport function.

Key Words: Seeing and Hearing Mechanism, Biomechanics, Measurement, Acoustic, Sound, Outer Hair Cell, Motor Protein, Prestin, Mutagenesis

1. Introduction

Outer hair cells (OHCs) in the mammalian organ of Corti elongate and contract in response to the change of their membrane potential, this OHC motility being generally referred to as electromotility[1]–[3]. The electromotility amplifies the vibration of organ of Corti (Fig. 1) and this amplification mechanism realizes the high sensitivity and sharp tuning of the auditory system[4]. It is inferred that the OHC is a direct voltage-to-force converter without dependence on ATP and can operate at microsecond rates[3]. The OHC motility is accompanied by a charge movement that can be recorded as nonlinear capacitance

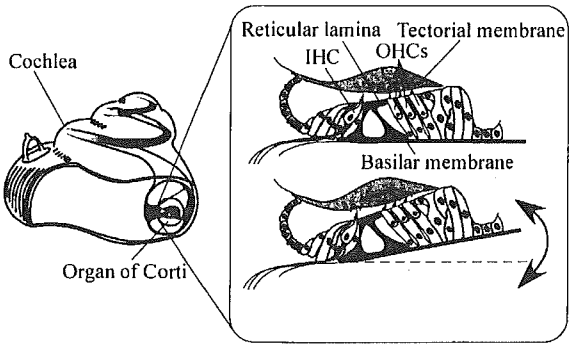

Fig. 1 Schematic of the cochlea and a cross section of the organ of Corti. When the basilar membrane is vibrated, shear motion between the tectorial membrane and the reticular lamina is evoked. Due to the deflection of the stereocilia of the IHC and OHCs, intracellular depolarization evoked by cation influx causes auditory nerve fiber activation of the IHC and simultaneously, the motile response applying force to the basilar membrane is produced in OHCs.

* Received 10th June, 2005 (No. 05-4072)
** Department of Bioengineering and Robotics, Tohoku University, 6–6–01 Aoba-yama, Sendai 980–8579, Japan. E-mail: wada@cc.mech.tohoku.ac.jp
*** Department of Medical Genome Sciences, The University of Tokyo, 5–1–5 Kashiwanoha, Kashiwa 277–8561, Japan
**** Department of Otorhinolaryngology, Juntendo University School of Medicine, 2–1–1 Hongo, Bunkyo-ku, Tokyo 113–8431, Japan
† Department of Biomolecular Engineering, Tohoku University, 6–6–07 Aoba-yama, Sendai 980–8579, Japan
†† Department of Otolaryngology, Head and Neck Surgery, Tohoku University Graduate School of Medicine, 1–1 Seiryo-machi, Sendai 980–8575, Japan

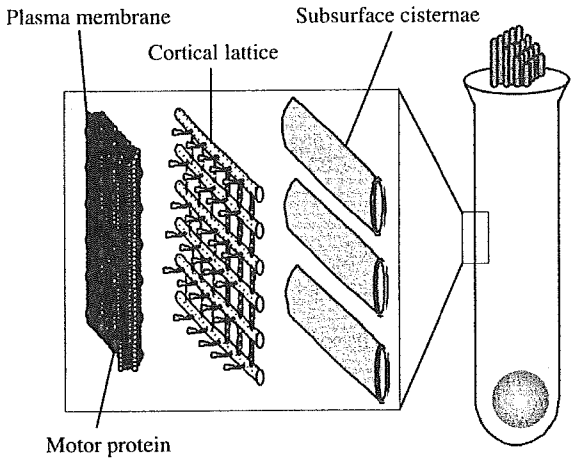

Fig. 2 Lateral wall of the OHC. The OHC lateral wall has a unique trilaminate structure: the outermost plasma membrane, the cortical lattice and the innermost subsurface cisternae. The motor protein is thought to be embedded in the plasma membrane.

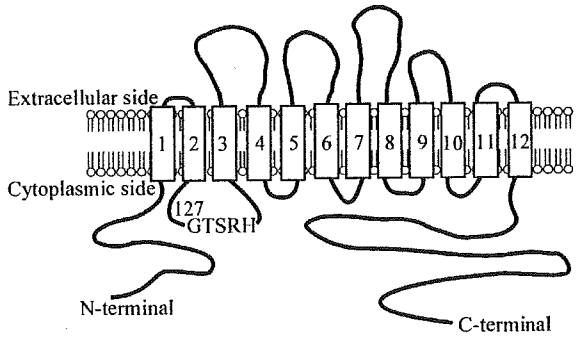

Fig. 3 Predicted membrane topology of prestin. It is considered that prestin has 12 transmembrane domains and that the N-terminus and C-terminus of prestin are located in the cytoplasm[9),16)]. The GTSRH sequence is at position 127–131 of prestin. The membrane topology was drawn based on the Swiss-Prot/TrEMBL database.

(NLC)[5)]. The source of the somatic length change of the OHCs is considered to be the conformational changes of a motor protein in the lateral plasma membrane of the OHCs[6),7)] (Fig. 2). In 2000, this motor protein was identified in the gerbil cochlea and termed prestin[8)].

As shown by amino acid sequence analyses, prestin consists of 744 amino acids with a molecular weight of about 81.4 kDa and is a member of the solute carrier (SLC) 26 family which transports anions through the cell membrane[8)] (Fig. 3). Mammalian cells transfected with prestin exhibit electromotility and NLC[8),9)]. By contrast, OHCs isolated from prestin knockout mice lack electromotility[10)]. From these results, prestin is believed to be the motor protein in the OHCs. However, the mechanism by which prestin functions has been unknown. For further clarification of that mechanism, it is necessary to elucidate the role of each amino acid of prestin.

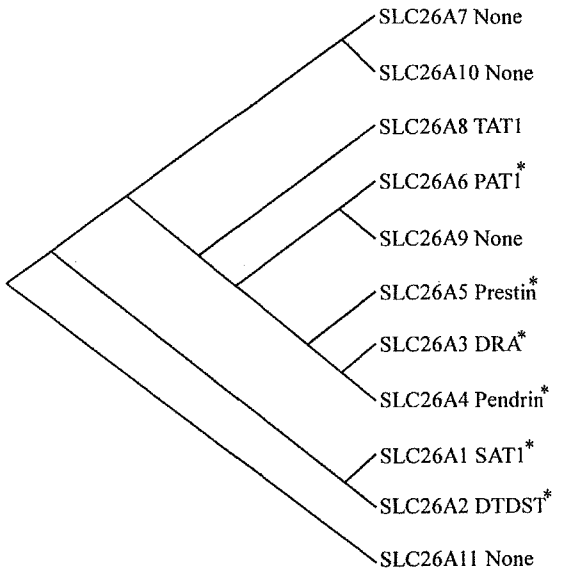

Fig. 4 Dendrogram of the SLC26 family. Human orthologs were used to generate a dendrogram with CLUSTALW. The GTSRH sequence is conserved in six proteins of the SLC26 family, which are indicated by asterisks. The amino acid sequences of the SLC26 family were obtained from the Swiss-Prot/TrEMBL database.

The GTSRH sequence of amino acids at positions 127–131 was completely conserved in six proteins of the SLC26 family (Fig. 4). In the case of pendrin, which is a member of the SLC26 family, substitution of threonine for serine in the GTSRH sequence is known to lead to syndromic hearing impairment[11)]. It is therefore likely that the GTSRH sequence is crucial for the SLC26 family. In this study, to clarify the role of the GTSRH sequence in the characteristics of prestin, alanine was substituted for glycine, threonine, serine, arginine and histidine individually and threonine was substituted for serine. Wild-type (WT) prestin and point mutants were expressed in human embryonic kidney (HEK) 293 cells. The expressions and localizations of WT prestin and the point mutants in HEK293 cells were then investigated by Western blotting and immunofluorescence experiments. Additionally, the membrane capacitance, which is an indicator of the anion transport function, of WT prestin and those of the point mutants were recorded by the whole-cell patch-clamp technique. By comparing the results for the WT prestin with those for the point mutants, the roles of the GTSRH sequence in the characteristics of prestin were examined.

2. Materials and Methods

2.1 Site-directed mutagenesis

The GTSRH sequence at positions 127–131 was altered, i.e., alanine was substituted for glycine, threonine, serine, arginine and histidine individually and thre-

Table 1 Primers used for site directed mutagenesis

Name	Sequence
5′ flanking forward	5′-CGGGATCCATGGATCATGCCGAAGAAAAATG-3′
3′ flanking reverse	5′-GGAATTCTTATGCCTCGGGTGTGGTGG-3′
3′ flanking FLAG reverse	5′-CCGCTCGAGTGCCTCGGGTGTGGTGGG-3′
G127A forward	5′-CTGTTTCTTTGCGACCTCCAGAC-3′
G127A reverse	5′-GTCTGGAGGTCGCAAAGAAACAG-3′
T128A forward	5′-GTTTCTTTGGGGCCTCCAGACAC-3′
T128A reverse	5′-GTGTCTGGAGGCCCCAAAGAAAC-3′
S129A forward	5′-CTTTGGGACCGCCAGACACATATC-3′
S129A reverse	5′-GATATGTGTCTGGCGGTCCCAAAG-3′
R130A forward	5′-CTTTGGGACCTCCGCACACATATCTATAG-3′
R130A reverse	5′-CTATAGATATGTGTGCGGAGGTCCCAAAG-3′
H131A forward	5′-GGGACCTCCAGAGCCATATCTATAGG-3′
H131A reverse	5′-CCTATAGATATGGCTCTGGAGGTCCC-3′
S129T forward	5′-CTTTGGGACCACCAGACACATATC-3′
S129T reverse	5′-GATATGTGTCTGGTGGTCCCAAAG-3′

onine was substituted for serine, resulting in six point mutants with the following sequences: ATSRH, GASRH, GTARH, GTSAH, GTSRA and GTTRH. These point mutants were constructed using overlap extension PCR with gerbil prestin cDNA inserted into the expression vector pIRES-hrGFP-1a (Stratagene, La Jolla, CA) as a template. Two separate PCRs were carried out with one flanking primer and one mutagenic primer which contained at least 23 bp homologous to that of other mutagenic primer (Table 1). For example, to construct the G127A mutant, one reaction solution contained a 5′ flanking forward primer and a G127A reverse primer, and the other solution contained a 3′ flanking reverse primer and a G127A forward primer. The two PCR products were purified from agarose gel after DNA electrophoresis, mixed together, and assembled by a primerless PCR. The assembled products were amplified with the two flanking primers. The resulting PCR product was gel purified and digested with *BamH*I and *EcoR*I (New England Biolabs, Beverly, MA). Digested products were ligated into *BamH*I and *EcoR*I sites of the expression vector.

To visualize prestin by using antibodies in Western blotting and immunofluorescence experiments, FLAG-tagged mutant prestin genes were constructed. The FLAG-tag sequence is downstream of the *Xho*I site in the pIRES-hrGFP-1a. Hence, to insert a mutant prestin gene between the *BamH*I and *Xho*I sites of the expression vector, a 3′ flanking FLAG reverse primer lacking the stop codon of prestin and having the *Xho*I site was used in overlap extension PCR. The resulting amplified products were gel purified and digested with *BamH*I and *Xho*I (New England Biolabs). Digested products were ligated into *BamH*I and *Xho*I sites of the expression vector. Each mutation was verified by an automated DNA sequencer (Applied Biosystems, Foster City, CA).

2.2 Cell culture and transfection

The difference of the characteristics between WT prestin and the point mutants can be clarified by using a cell line which does not express prestin. As the efficiencies of transfection and protein expression of HEK293 cells are high, this cell line was used for following experiments. HEK293 cells were cultured in RPMI-1640 medium with 10% fetal bovine serum, 100 U penicillin/mL and 100 μg streptomycin/mL at 37°C with 5% CO_2. One day before transfection, HEK293 cells were plated in 35-mm culture dishes. Constructed expression vectors were transfected into HEK293 cells using LipofectAMINE 2000 Reagent (Invitrogen, Rockville, MD) according to the manufacturer's instructions. As the transfected cells expressed green fluorescent protein (GFP) due to the GFP gene inserted into the expression vector, the introduction of the expression vectors was confirmed by GFP observation.

2.3 Western blotting

To confirm the expression of FLAG-tagged point mutants and the molecular weight of the expressed proteins, Western blotting was performed. The transiently transfected cells were dissolved in SDS sample buffer at a concentration of 1×10^5 cells/10 μL. After boiling for 5 min at 100°C, 10 μL of the cell lysates were electrophoresed on 10% polyacrylamide gel. Separated proteins in an SDS-PAGE were transferred to nitrocellulose membranes (Hybond-ECL, Amersham Biosciences, Uppsala, Sweden). The membranes were blocked by 5% skim milk in PBS containing 0.05% Tween20 (PBS-T). After blocking and PBS-T washing, the membranes were incubated with anti-FLAG mouse monoclonal antibody (Sigma-Aldrich, St. Louis, MO) in PBS-T. After incubation for 30 min at room temperature, the membranes were washed with PBS-T. The membranes were then incubated with HRP-conjugated anti-mouse IgG antibody

(Cell Signaling Technology, Beverly, MA) in PBS-T for 30 min at room temperature. The membranes were washed with PBS-T and then visualized by enhanced chemiluminescence using an ECL Western blotting detection kit (Amersham Biosciences). Western blotting images were obtained with a luminescent image analyzer (LAS-1000, FUJIFILM, Kanagawa, Japan).

2.4 Immunofluorescence experiments

To confirm the localization of FLAG-tagged point mutants, immunofluorescence experiments were performed. Transiently transfected HEK293 cells were fixed with 4% paraformaldehyde for 5 min at room temperature and washed with PBS. Non-specific binding was avoided by the addition of 50% Block Ace (Dainippon Pharmaceutical, Osaka, Japan) and 50% fetal bovine serum. After PBS washing, anti-FLAG antibody (Sigma-Aldrich) in PBS with 0.1% saponin solution was added to the cells. After incubation for 1 h at 37°C, the cells were washed with PBS and then incubated with TRITC-conjugated anti-mouse IgG antibody (Sigma-Aldrich) in PBS with 0.1% saponin solution for 30 min at 37°C. After PBS washing, the stained cells were observed using a confocal laser scanning microscope (FV500, Olympus, Tokyo, Japan).

2.5 Electrophysiological experiments

Prestin-expressing cells exhibit bell-shaped NLC in response to the change of membrane potential[6),(8),(9)]. As NLC shows a voltage-dependent charge transfer of prestin, the anion transport function of prestin was evaluated with NLC measured by the whole-cell patch-clamp technique. For patch-clamp measurements, the transiently transfected HEK293 cells in a culture dish were transferred to several glass-base dishes (IWAKI, Chiba, Japan). Electrodes were pulled from the borosilicate glass tube (TW150-4, World Precision Instruments, Inc., Sarasota, FL) by a programmable pullar (Model P-97, Sutter Instruments Co., Novato, CA), and had resistances between 2 and 5 MΩ. Electrodes were filled with an internal solution with the following composition: 140 mM CsCl, 2 mM $MgCl_2$, 10 mM EGTA and 10 mM HEPES, pH adjusted to 7.2 with CsOH. The external medium had the following composition: 120 mM NaCl, 20 mM TAE-Cl, 2 mM $CoCl_2$, 2 mM $MgCl_2$, 10 mM HEPES and 5 mM glucose, pH adjusted to 7.2 with NaOH.

The measurement system consists of a patch amplifier (Axopatch 200B amplifier, Axon Instruments, Foster City, CA), an A/DD/A converter (Digidata 1320A, Axon Instruments), a personal computer and a function generator (WF1944, NF Electronic Instruments, Kanagawa, Japan). Measurements of membrane capacitance were performed using the "membrane test" feature of pCLAMP 8.0 acquisition software (Axon Instruments). A test square wave (amplitude, 20 mV; period $T = 4$ msec, i.e., frequency, 250 Hz) was generated by the personal computer controlled by pCLAMP 8.0 software and applied to the cell through the amplifier. The transient current, which is caused by the test square wave, was then sampled through the amplifier. Transient current Q, current decay τ and total resistance R_t were continuously calculated by pCLAMP 8.0 software at a resolution of 25 Hz, by averaging the responses to 10 positive and 10 negative consecutive test steps, and measured values of these parameters were stored in the computer. Access resistance R_a, membrane resistance R_m and membrane capacitance C_m were then obtained by substituting Q, τ and R_t into the following equations[6)]:

$$R_a = \frac{R_t \tau V_c}{Q R_t + \tau V_c}, \tag{1}$$

$$R_m = R_t - R_a, \tag{2}$$

$$C_m = \left(\frac{R_t}{R_m}\right)^2 \frac{Q}{V_c}, \tag{3}$$

where V_c is a voltage step. To determine the voltage dependence of membrane capacitance, triangular voltage ramps were superimposed on the above-mentioned square test wave. This triangular voltage wave (period $T = 2$ sec) was generated by the function generator and swung the cell potential from −140 mV to +70 mV[12)]. After the measurements, the membrane capacitance was plotted versus the membrane potential.

The membrane capacitance recorded from prestin-expressing cells was fitted to the derivative of the Boltzmann function[5)],

$$C_m(V) = C_{lin} + \frac{Q_{max}}{\alpha e^{\frac{V-V_{1/2}}{\alpha}} \left(1 + e^{-\frac{V-V_{1/2}}{\alpha}}\right)^2}, \tag{4}$$

where C_{lin} is the linear capacitance, Q_{max} is the maximum charge transfer, V is the membrane potential and $V_{1/2}$ is the voltage at half-maximal charge transfer. In Eq. (4), α is the slope factor of the voltage-dependent charge transfer and is given by

$$\alpha = kT/ze, \tag{5}$$

where k is Boltzmann's constant, T is absolute temperature, z is valence and e is electron charge. The software program KaleidaGraph (Synergy Software, Reading, PA) was used for data analysis and curve fitting. To evaluate the expression level of prestin in the unit cell membrane, Q_{max}, which reflects the expression level of prestin in whole cell membrane, was normalized and designated as charge density. The normalization was achieved by division of Q_{max} by C_{lin}, which is proportional to the membrane area of the cells. The unit of charge density is fC/pF.

3. Results

3.1 Expression and molecular weight of the point mutants

Western blotting was performed in order to confirm the expression of FLAG-tagged point mutants and the

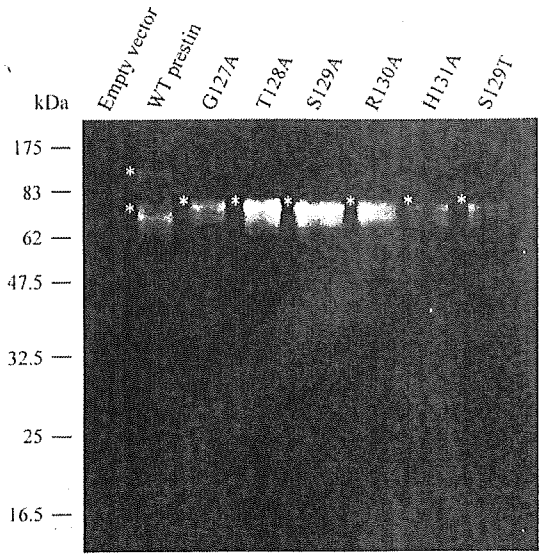

Fig. 5 Results of Western blotting. There was no band in the HEK293 cells transfected with the empty vector. Two major bands of about 100 kDa and 70 kDa were observed in HEK293 cells transfected with FLAG-tagged WT prestin. One major band of about 80 kDa was observed in HEK293 cells transfected with FLAG-tagged point mutants. Asterisks indicate the major bands.

molecular weight of the expressed proteins in HEK293 cells. The results of Western blotting of HEK293 cells transfected separately with an empty vector, FLAG-tagged WT prestin or FLAG-tagged point mutants are shown in Fig. 5. Major bands are indicated by asterisks. There was no band in HEK293 cells transfected with the empty vector. Two major bands of about 100 kDa and 70 kDa were detected in HEK293 cells transfected with FLAG-tagged WT prestin. One major band of about 80 kDa was detected in HEK293 cells transfected with FLAG-tagged point mutants.

3.2 Localization of the point mutants

The localization of FLAG-tagged point mutants in HEK293 cells was examined by immunofluorescence experiments. After confirming the introduction of the expression vectors by GFP observation, cell morphology and TRITC staining was observed. The differential and immunofluorescence images of HEK293 cells separately transfected with the empty vector, FLAG-tagged WT prestin or FLAG-tagged point mutants are shown in Fig. 6. HEK293 cells transfected with the empty vector were not stained. In the case of FLAG-tagged WT prestin and FLAG-tagged point mutants except for T128A, the membrane of transfected cells was stained. By contrast, in the case of FLAG-tagged T128A, both cell membrane and cytoplasm, except for the nucleus, were stained.

3.3 Functional evaluation of the point mutants

To evaluate the anion transport function of the point

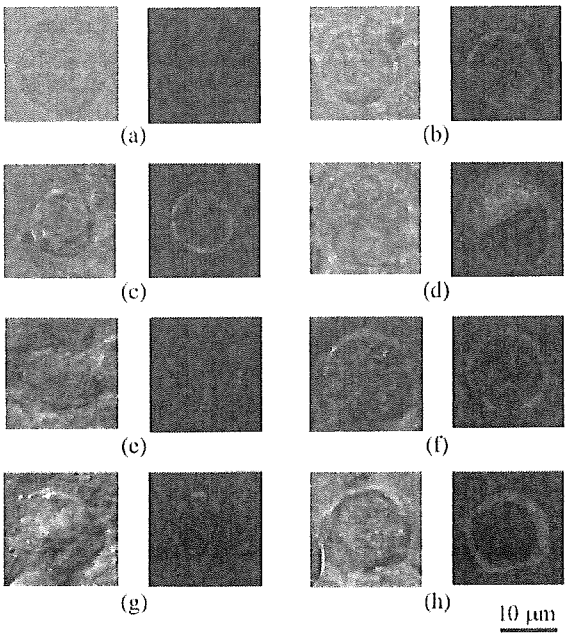

Fig. 6 Differential and immunofluorescence images of HEK293 cells separately transfected with WT prestin or the point mutants. (a) Empty vector. (b) WT prestin. (c) G127A. (d) T128A. (e) S129A. (f) R130A. (g) H131A. (h) S129T. HEK293 cells separately transfected with WT prestin or the point mutants except T128A were stained in the cell membrane. By contrast, HEK293 cells transfected with T128A were stained not only in the cell membrane but also in the cytoplasm.

mutants, whole-cell patch-clamp technique was used. To estimate the NLC of unit cell surface, the normalized nonlinear capacitance $C_{\mathrm{nonlin/lin}}$ was defined as

$$C_{\mathrm{nonlin/lin}}(V) = \frac{C_{\mathrm{nonlin}}}{C_{\mathrm{lin}}} = \frac{(C_{\mathrm{m}}(V) - C_{\mathrm{lin}})}{C_{\mathrm{lin}}}, \qquad (6)$$

where C_{nonlin} is the nonlinear component of the measured membrane capacitance. Furthermore, to compare the normalized data of the point mutants with that of the WT prestin, $C_{\mathrm{nonlin/lin}}(V)$ was divided by the maximum $C_{\mathrm{nonlin/lin}}(V)$ of WT prestin and termed relative $C_{\mathrm{nonlin/lin}}(V)$. Relative $C_{\mathrm{nonlin/lin}}(V)$ plots are shown in Fig. 7. Data points were fitted to Eq. (4), results of the fitting being shown by solid or dashed lines. WT prestin ($n = 49$), G127A ($n = 6$), T128A ($n = 4$), S129A ($n = 5$) and R130A ($n = 7$) exhibited the NLC versus membrane potential. On the other hand, the membrane capacitance of cells expressing H131A ($n = 11$) or S129T ($n = 4$) versus membrane potential was constant, similar to the data from the cells transfected with the empty vector. Fitting parameters are shown in Table 2. The charge density, α, and $V_{1/2}$ of the point mutants were compared with that of WT prestin and are shown in Fig. 8. There are statistical differences in charge density between WT prestin and G127A, T128A, S129A or R130A, in α between WT prestin and G127A or R130A and in $V_{1/2}$ between WT prestin and G127A.

Table 2 Fitting parameters for WT prestin and the point mutants

Gene	Charge density (fC/pF)	C_{lin} (pF)	Q_{max} (fC)	α (mV)	$V_{1/2}$ (mV)
WT prestin (n = 49)	20.0 ± 9.6	15.0 ± 5.4	229.6 ± 157.3	30.7 ± 3.7	-62.3 ± 9.2
G127A (n = 6)	7.2 ± 1.2	11.9 ± 1.9	87.6 ± 27.0	43.4 ± 5.0	28.5 ± 11.2
T128A (n = 4)	3.0 ± 1.6	15.0 ± 3.9	47.3 ± 31.3	37.0 ± 6.1	-72.3 ± 10.7
S129A (n = 5)	3.5 ± 1.5	13.4 ± 1.9	47.8 ± 25.1	36.7 ± 5.0	-55.2 ± 15.7
R130A (n = 7)	7.2 ± 6.7	19.4 ± 11.4	114.3 ± 78.5	36.6 ± 5.2	-69.6 ± 11.9

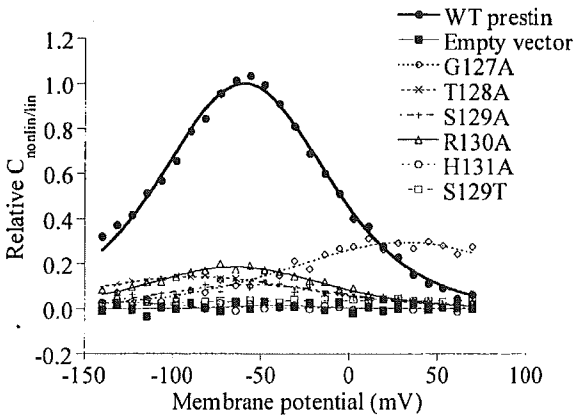

Fig. 7 Representative data of membrane capacitance versus membrane potential. Normalized nonlinear capacitance is divided by the maximum value of the normalized nonlinear capacitance of the WT prestin. Data points were fitted to Eq. (4), which is shown by the solid or dashed lines. WT prestin (n = 49), G127A (n = 6), T128A (n = 4), S129A (n = 5) and R130A (n = 7) exhibited NLC. On the other hand, the empty vector, H131A (n = 11) and S129T (n = 4) did not exhibit it. Fitting parameters for WT prestin were as follows: charge density = 19.3 fC/pF, Q_{max} = 321.6 fC, α = 31.2 mV and $V_{1/2}$ = −59.6 mV; for G127A: charge density = 8.3 fC/pF, Q_{max} = 101.4 fC, α = 45.1 mV and $V_{1/2}$ = 32.0 mV; for T128A: charge density = 3.8 fC/pF, Q_{max} = 58.5 fC, α = 42.1 mV and $V_{1/2}$ = −87.0 mV; for S129A: charge density = 2.4 fC/pF, Q_{max} = 34.5 fC, α = 36.3 mV and $V_{1/2}$ = −54.9 mV; for R130A: charge density = 3.9 fC/pF, Q_{max} = 66.1 fC, α = 33.6 mV and $V_{1/2}$ = −64.2 mV.

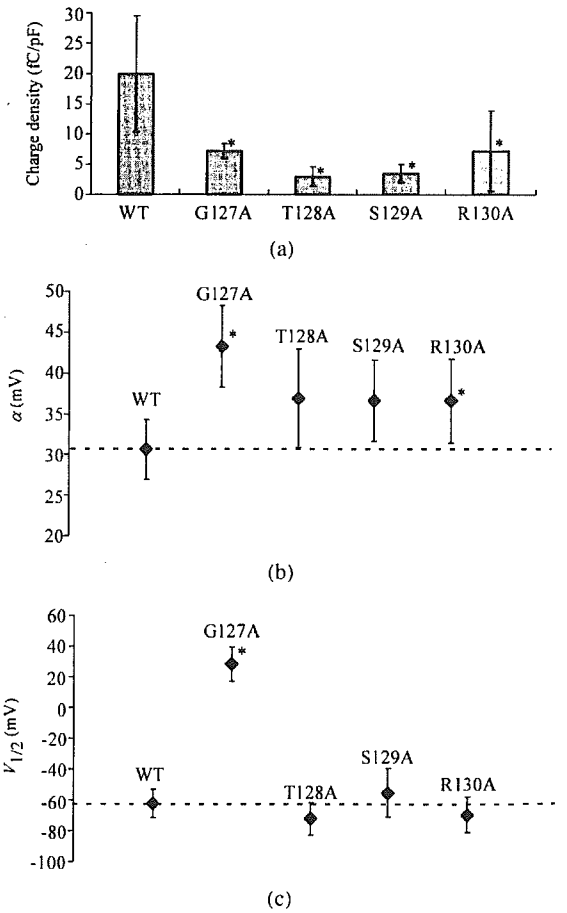

Fig. 8 Fitting parameter variation for the point mutants. (a) Charge density of WT prestin and the point mutants. The charge densities of all point mutants were lower than that of WT prestin, and there was a statistical difference. (b) α of WT prestin and the point mutants. There was a statistical difference between α of WT prestin and those of the G127A and the R130A. (c) $V_{1/2}$ of WT prestin and the point mutants. Only G127A displayed a statistical significant shift of $V_{1/2}$ to the depolarizing side. Asterisks represent significance vs. WT prestin ($p < 0.05$).

4. Discussion

As shown in Fig. 5, no band appeared in the HEK293 cells transfected with the empty vector. This result suggests that the band which appeared in the other transfected cells showed only prestin. The theoretical molecular weights of FLAG-tagged WT prestin and FLAG-tagged point mutants are 84.6 kDa. However, the results of Western blotting show two major bands of about 100 kDa and 70 kDa in the cells transfected with WT prestin as shown in Fig. 5. In general, there are two major types of N-linked carbohydrates: complex oligosaccharides and high-mannose oligosaccharides. It is considered that the 100 kDa band detected in the presnt study indicates prestin glycosylated with complex-type oligosaccharides and the 70 kDa band indicates prestin glycosylated

with high-mannose-type oligosaccharides and unglycosylated prestin. The broadness of the band detected around 100 kDa is considered to be due to the variation in the size of carbohydrate chains. On the other hand, the band detected around 70 kDa was also broad. As the molecular mass of prestin glycosylated with high-mannose-type oligosaccharides is close to that of unglycosylated prestin, two bands of these proteins may overlap. As a result, the band detected around 70 kDa may be broad. It has been reported that one gycosylated prestin band of about 106 kDa in WT prestin-expressing TSA201 cells, which are derivatives of the HEK293 cell line, was observed and that the band shifted from about 106 kDa to about 72 kDa after deglycosylation, suggesting 72 kDa of unglycosylated prestin[13]. Our results agree with the previous report.

An unglycosylated prestin band appeared at a position lower than the theoretical molecular weight. This result is possibly attributable to the high content of hydrophobic amino acid residues in the membrane protein. More negatively charged sodium dodecyl sulphate (SDS) binds to the hydrophobic amino acids residues of membrane proteins than average soluble proteins and this complex was pulled toward the positive electrode, resulting in faster gel migration.

One major band of about 80 kDa was observed in the cells transfected with the point mutants. The 80 kDa bands of the point mutants as well as the 70 kDa band of WT prestin may indicate prestin glycosylated with high-mannose-type oligosaccharides and unglycosylated prestin. The reason why the feature of the band of the point mutants is different from that of the 70 kDa band of WT prestin may be the difference between the expression level of prestin glycosylated with high-mannose-type oligosaccharides and that of unglycosylated prestin, i.e., cells transfected with WT prestin expressed unglycosylated prestin more than prestin glycosylated with high-mannose-type oligosaccharides and vice versa in the cells transfected with the point mutants.

As shown in Fig. 6, in the results of immunofluorescence experiments, TRITC staining was not observed in HEK293 cells transfected with the empty vector. This result suggests that anti-FLAG antibody recognized only prestin. Hence, the results of immunofluorescence experiments showed that G127A, S129A, R130A, H131A and S129T were expressed in the cell membrane as WT prestin and that T128A was expressed in both the cell membrane and the cytoplasm. As the substitution of alanine for threonine is least likely to disturb the protein structure[14], the change of the localization of T128A is not thought to have been due to the misfolding of T128A. This implies that Thr-128 may play a crucial role in the membrane targeting process. By contrast, the substitution of alanine for glycine, serine, arginine and histidine did not affect this process.

In the whole-cell patch-clamp technique, NLC was not obtained from HEK293 cells transfected with H131A. This result means that H131A lost the anion transport function in HEK293 cells. Bordo and Argos reported that a disturbance of the protein fold possibly occurs due to the substitution of any other amino acid for histidine[14]. This may suggest that histidine is an amino acid which is essential for maintaining any protein structure. Hence, the loss of the anion transport function of H131A may suggest that His-131 is important for protein folding in prestin as well as in other proteins.

In the case of pendrin, substitution of threonine for serine in the GTSRH sequence has been found to cause syndromic hearing impairment[11]. To reveal the effect of the substitution of threonine for serine in the GTSRH sequence on the characteristics of prestin, not only alanine but also threonine was substituted for Ser-129. NLC was not obtained from HEK293 cells transfected with S129T, i.e., S129T lost its anion transport function in HEK293 cells. The difference between serine and threonine is only the presence of an extra methyl group in threonine. Due to the presence of this group, position 129 of prestin sterically excludes threonine. Furthermore, although the NLC was obtained from HEK293 cells transfected with S129A, the charge density was less than that of WT prestin. The charge density reflects the amount of charge transfer in the unit cell surface. The reduction of the charge density of the point mutant was the result of a decrease in the number of functional prestin molecules at the unit cell membrane or a decline in the amount of charge transfer by unit prestin. The only difference between serine and alanine is the presence of the hydroxyl group in serine. It was therefore considered that the hydroxyl group of serine is essential for the anion transport function of prestin or maintaining its structure.

As is the case with S129A, although the NLC was obtained from HEK293 cells separately transfected with G127A, T128A or R130A, the charge density of these mutants was less than that of WT prestin. Since the substitution of alanine for glycine was expected to maintain the protein fold, the reduction of the charge density might not be due to the misfolding of G127A. There were statistical differences in α and $V_{1/2}$ between WT prestin and G127A. The α is a slope factor which characterizes voltage-dependent membrane capacitance and also shows the properties of the anion binding and transport[15]. The larger value of α shows that a larger potential change is necessary for anion binding and for translocating anions across a cell membrane. The $V_{1/2}$ is the voltage at which charges are moved with the smallest voltage-increment. The shift of $V_{1/2}$ indicates that the point changes at which prestin is sensitive for the membrane potential. The α of G127A was significantly larger than that of WT prestin

and the $V_{1/2}$ of G127A was remarkably shifted in the depolarization direction. These results suggest that Gly-127 is associated with anion binding and transport. Furthermore, a multiple amino acid sequence alignment of eleven proteins of the SLC26 family showed that Gly-127 is conserved in all proteins of the SLC26 family, although other amino acids in the GTSRH sequence are conserved in six to eight proteins of this family. This fact also supports the idea that Gly-127 is critical for anion binding and transport of prestin.

Although WT prestin is a membrane protein which transport anions via the cell membrane, prestin expressed in cytoplasm cannot sense the change of membrane potential and cannot transport anions via the cell membrane. In Thr-128, as T128A was expressed in both the cell membrane and cytoplasm, the reduction of its charge density may be due to the decrease in the number of functional prestin molecules at the unit cell membrane. In Arg-130, since it is conceivable that the substitution of alanine for arginine does not maintain the protein structure[14], the reduction of charge density of the R130A is possibly due to R130A being in a misfolded state. However, as R130A exhibits NLC, the degree of misfolding is not as serious as that of H131A.

5. Conclusion

To reveal the role of the GTSRH sequence of prestin at positions 127–131 in the characteristics of prestin, mutational analysis was performed. The results show that the GTSRH sequence plays an important role in the localization of prestin, as well as in its anion transport function.

Acknowledgments

This work was supported by a grant from the Human Frontier Science Program, by a Health and Labour Science Research Grant from the Ministry of Health, Labour and Welfare of Japan, and by Grant-in-Aid for Scientific Research on Priority Areas 15086202 from the Ministry of Education, Culture, Sports, Science and Technology of Japan.

References

(1) Brownell, W.E., Basder, D. and Ribaupierre, Y., Evoked Mechanical Responses of Isolated Cochlear Outer Hair Cells, Science, Vol.227 (1985), pp.94–196.

(2) Kachar, B., Brownell, W.E., Altschuler, R. and Fex, J., Electrokinetic Shape Changes of Cochlear Outer Hair Cells, Nature, Vol.322 (1986), pp.365–368.

(3) Ashmore, J.F., A Fast Motile Response in Guinea-Pig Outer Hair Cells: The Cellular Basis of the Cochlear Amplifier, J. Physiol., Vol.388 (1987), pp.323–347.

(4) Dallos, P., The Active Cochlea, J. Neurosci., Vol.12 (1992), pp.4575–4585.

(5) Santos-Sacchi, J., Reversible Inhibition of Voltage-Dependent Outer Hair Cell Motility and Capacitance, J. Neurosci., Vol.11 (1991), pp.3096–3110.

(6) Huang, G. and Santos-Sacchi, J., Mapping of the Distribution of the Outer Hair Cell Motility Voltage Sensor by Electrical Amputation, Biophys. J., Vol.65 (1993), pp.2228–2236.

(7) Forge, A., Structural Feature of the Lateral Walls in Mammalian Cochlea Outer Hair Cells, Cell Tissue Res., Vol.265 (1991), pp.473–485.

(8) Zheng, J., Shen, W., He, D.Z.Z., Long, K.B., Madison, L.D. and Dallos, P., Prestin Is the Motor Protein of Cochlear Outer Hair Cells, Nature, Vol.405 (2000), pp.149–155.

(9) Ludwjg, J., Oliver, D., Frank, G., Klöcker, N., Gummer, A.W. and Fakler, B., Reciprocal Electromechanical Properties of Rat Prestin: The Motor Molecule from Rat Outer Hair Cells, Proc. Natl. Acad. Sci. U.S.A., Vol.98 (2001), pp.4178–4183.

(10) Liberman, M.C., Gao, J., He, D.Z.Z., Wu, X., Jia, S. and Zuo, J., Prestin Is Required for Electromotility of the Outer Hair Cell and for the Cochlear Amplifier, Nature, Vol.419 (2002), pp.300–304.

(11) Fugazzola, I., Cerutti, N., Mannavola, D., Crino, A., Gasparoni, P., Vannucchi, G. and Beck-Peccoz, P., Differential Diagnosis between Pendred and Pseudo-Pendred Syndromes: Clinical, Radiologic, and Molecular Studies, Pediatr. Res., Vol.51 (2002), pp.479–484.

(12) Frolenkov, G.I., Mammano, F., Belyantseva, I.A., Coling, D. and Kachar, B., Two Distinct Ca^{2+}-Dependent Signaling Pathways Regulate the Motor Output of Cochlear Outer Hair Cells, J. Neurosci., Vol.20 (2000), pp.5940–5948.

(13) Matsuda, K., Zheng, J., Du, G.G., Klocker, N., Madison, L.D. and Dallos, P., N-Linked Glycosylation Sites of the Motor Protein Prestin: Effects on Membrane Targeting and Electrophysiological Function, J. Neurochem., Vol.89 (2004), pp.928–938.

(14) Bordo, D. and Argos, P., Suggestions for "Safe" Residue Substitutions in Site-Directed Mutagenesis, J. Mol. Bio., Vol.217 (1991), pp.721–729.

(15) Oliver, D., He, D.Z.Z., Klöcker, N., Ludwig, J., Schulte, U., Waldegger, S., Ruppersberg, J.P., Dallos, P. and Bernd, F., Intracellular Anions as the Voltage Sensor of Prestin, the Outer Hair Cell Motor Protein, Science, Vol.292 (2001), pp.2340–2343.

(16) Zheng, J., Long, K.B., Shen, W., Madison, L.D. and Dallos, P., Prestin Topology: Localization of Protein Epitopes in Relation to the Plasma Membrane, Neuroreport, Vol.12 (2001), pp.1929–1935.